

1 Title: Over two orders of magnitude difference in rate of single chromosome loss among sundew
2 (*Drosera* L., Droseraceae) lineages
3

4 Running Head: Rate of chromosome evolution in *Drosera*
5

6 Authors: Rebekah A. Mohn^{1*}, Rosana Zenil-Ferguson², Thilo A. Krueger³, Andreas S.
7 Fleischmann^{4,5}, Adam T. Cross^{3,6}, Ya Yang¹
8

9 Affiliations:

10 ¹Department of Plant and Microbial Biology, University of Minnesota-Twin Cities, 1445 Gortner Avenue, St. Paul,
11 MN 55108-1095, United States of America

12 ²Department of Biology, University of Hawai'i Mānoa, Mānoa, Hawai'i

13 ³School of Molecular and Life Sciences, Curtin University, Bentley, Australia

14 ⁴Botanische Staatssammlung München (SNSB-BSM), Munich, Germany

15 ⁵GeoBio-Center LMU, Ludwig-Maximilians-University, Munich, Germany

16 ³School of Molecular and Life Sciences, Curtin University, Bentley, Australia

17 ⁶EcoHealth Network, Brookline, Massachusetts, United States of America.

18 *Corresponding author's email: rebekah.mohn@gmail.com
19

20 Author Contribution Statement: RM designed and led the work. TK, AF, and AC contributed to
21 literature search and verified taxonomy. RM and RZF analyzed the data. RM and YY led the
22 writing. All authors provided feedback on the manuscript and approved the final version.
23

24 Abstract:

25 Chromosome number change is a driver of speciation in eukaryotic organisms. Carnivorous
26 sundews, the plant genus *Drosera* L., exhibit single chromosome number variation among and
27 within species, especially in the Australian *Drosera* subg. *Ergaleium* D.C., potentially linked to
28 the presence of holocentromeres. We reviewed literature, verified chromosome counts, and using
29 an *rbcL* chronogram, tested alternate models where the gain, loss, and doubling rates (+1, -1,
30 $\times 2$) were the same or different between *D.* subg. *Ergaleium* and the other subgenera. Ancestral
31 chromosome number estimations were performed, and the distributions of self-compatibility and
32 genome size were visualized across the genus. The best model for chromosome evolution had
33 equal rates of polyploidy (0.014 per million years; Myr) but higher rates of single chromosome
34 number gain (0.19 and 0.027 per Myr) and loss (0.23 and 0.00059 per Myr) in *D.* subg.
35 *Ergaleium* compared to the other subgenera. We found no evidence for differences in single
36 chromosome evolution to be due to differences in diploidization after polyploidy or to
37 holocentromeres as had been proposed. This study highlights the complexity of factors
38 influencing rates of chromosome number evolution.
39

40 Keywords: BiChrom model; chromosome number change; diploidization; RevBayes;
41 holocentromeres; carnivorous plants
42

43 Data Accessibility: All data not available in the supplementary material will be archived and
44 made available at DOI:10.5281/zenodo.6081366 upon manuscript acceptance for publication.
45

46 Acknowledgements:

47 The authors thank Fernando Rivadavia for his voucher identification and feedback on the
48 manuscript, Alex Eilts and the College of Biological Sciences Conservatory for their assistance
49 in growing plants for genome size estimation, Aaron Lee for his feedback on the manuscript, the
50 University of Western Australia library for access to Lin Chen's Thesis, Sergey Matveev for help
51 with Russian translation, and Virginia's Department of Conservation and Recreation and Darren
52 Loomis for access and help obtaining specimens to the Cherry Orchard Bog Natural Area
53 Preserve. The work is supported by the National Science Foundation (Grant Number: 2015210),
54 the Fulbright Futures Program, and the Botanical Society of America.
55
56 Conflict of Interests: The authors have no conflict of interests to declare.

57 Chromosome evolution events, such as duplication, inversion, fusion, and fission, are universal
58 across the eukaryotic tree of life but appear to be more common in some lineages than others
59 (reviewed in Coglan et al., 2005). These chromosomal changes have long been considered
60 driving forces of speciation and lineage diversification (Stebbins, 1971; Grant, 1981; Coyne and
61 Orr, 2004). Therefore, identifying lineages with unusual rates of chromosome change and the
62 intrinsic and environmental factors influencing these rates is critical to our understanding of
63 evolutionary processes in general.

64
65 Recent developments in macroevolutionary modeling approaches have explored the association
66 of chromosome evolution with trait evolution and lineage diversification (Mayrose et al., 2011;
67 Freyman and Höhna, 2018; Baniaga et al., 2019; Zenil-Ferguson et al., 2019; Román-Palacios et
68 al., 2020; Zhan et al., 2021). However, most of this work has focused on the role of chromosome
69 doubling. Putative factors influencing the occurrence of single chromosome change include post-
70 polyploidy dysploidy and rediploidization (Mandáková and Lysák, 2018), as well as centromere
71 type (Luceño and Guerra, 1996; Mayrose and Lysák, 2020; Ruckman et al., 2020). Factors
72 influencing the establishment of a new karyotype, such as autogamy (selfing) and clonality in
73 plants, have only been explored in relation to polyploidy but likely impact single chromosome
74 evolution as well (Husband et al., 2013; Weiss-Schneeweiss et al., 2013; Van Drunen and
75 Husband, 2019). The relative importance of selfing and clonality in single chromosome
76 evolution and establishment remains largely unknown.

77
78 Despite the importance of chromosome change to understanding evolution, obtaining a dataset of
79 chromosome numbers with a matching phylogenetic tree to model the rates of chromosome
80 change is challenging. A well-resolved phylogeny with a comprehensive species-level sampling
81 is not always available. Further, because fresh root tips or flower buds are required to obtain
82 chromosome counts, chromosome counts are often incomplete for lineages with wide geographic
83 distributions. In addition to incomplete sampling, the quality of chromosome count datasets is
84 eroded by chromosome counting errors (Windham and Yatskievych, 2003), reporting errors in
85 chromosome number databases (Rivero et al., 2019), and taxonomic uncertainty from species
86 misidentifications or taxonomic changes.

87
88 The carnivorous plants known as sundews (genus *Drosera* L.; family Droseraceae; order
89 Caryophyllales) are exceptionally well-studied cytologically, with chromosome counts available
90 for about half of its ca. 260 species. *Drosera* species are widely distributed and occur in a wide
91 variety of habitats from boreal peatlands to tropical savannahs and subtropical sandplain
92 heathlands and rock outcrops (Fleischmann et al., 2018). Hotspots of species diversity include
93 Australia (ca. 170 species), Africa (ca. 40 species), and South America (ca. 40 species;
94 Fleischmann et al., 2018). *Drosera* consists of four well-supported subgenera (Fleischmann et
95 al., 2018): the two early-branching *D.* subg. *Regiae* Seine & Barthlott and *Arcturia* (Planch.)
96 Schlauer harbor only one and two species respectively, while the sister *D.* subg. *Drosera* L. and
97 *Ergaleium* D.C. are species-rich and harbor ca. 110 and ca. 150 species, respectively.
98 Cytological studies on *Drosera* have been undertaken for over 120 years (Huie, 1897;
99 Rosenberg, 1903), resulting in a rich literature record comprising more than 600 individual
100 chromosome counts for ca. 140 species (e.g., Rothfels and Heimburger, 1968; Kress, 1970;
101 Sheikh and Kondo, 1995; Chen, 1998; Rivadavia, 2005).

103 Previous karyotype studies in *Drosera* have revealed strikingly elevated levels of single
104 chromosome number variation in *D. subg. Ergaleium* (almost every number from $n = 3$ to 23,
105 with numbers up to 45; tuberous, pygmy, and woolly sundews of Australia; Table S1; Sheikh
106 and Kondo 1995; Hoshi and Kondo, 1998; Rivadavia et al., 2003; Shirakawa, Hoshi, et al.,
107 2011). In contrast, the other three subgenera exhibit primarily polyploid chromosome variation
108 (Hoshi and Kondo, 1998; Rivadavia et al., 2003). The increased single chromosome number
109 variation has been attributed to the presence of holocentric chromosomes in *Drosera* (Sheikh et
110 al., 1995). Holocentric chromosomes have a centromere along their entire length rather than
111 localized in the typical, X-shaped, monocentric chromosome. Because chromosomes of all
112 *Drosera* except *D. regia* (Shirakawa, Nagano, et al., 2011) and *D. slackii* (Bennett and Cheek,
113 1990) lack a visible centromere constriction (Nontachaiyapoom et al., 2000; Kondo and
114 Nontachaiyapoom, 2008), and all eight species tested so far undergo successful mitotic
115 segregation after breakage (Sheikh et al., 1995; Furuta and Kondo, 1999; Shirakawa, Hoshi, et
116 al., 2011; Zedek et al., 2016; Kolodin et al., 2018), researchers have hypothesized
117 holocentromeres to be present in almost all *Drosera*. However, the distribution of phospho-
118 histone 2A threonine-120, a histone commonly associated with the centromeric and pericentric
119 region (Dong and Han, 2012; Wanner et al., 2015), indicates monocentromeres in three species
120 from *D. subg. Drosera* and *D. subg. Ergaleium* (Demidov et al., 2014). Together, the evidence
121 suggests that holocentromeres do not correspond to higher levels of chromosome number
122 variation in *Drosera*. However, contrasting levels of chromosome number variation could also
123 result from different ages of the lineages, uneven taxon sampling, counting errors, and taxonomic
124 misidentification of material used for counts (e.g., the confusion of *D. aliciae* and *D. spatulata*;
125 see Kress 1970; of *D. montana* and closely allied taxa; see Rivadavia, 2005). A critical
126 evaluation of chromosome count data quality across all records is required to lay the foundations
127 for subsequent analyses. Furthermore, the rate of chromosome number change has yet to be
128 tested using a modeling framework that considers both the phylogenetic history and different
129 modes of chromosome evolution. This phylogenetic modeling framework would also allow the
130 investigation of associations between rates of chromosome number evolution and traits such as
131 centromere type, life history, clonal propagation, and mating system.
132

133 In this study, we quantified the rate of chromosome doubling and single chromosome gain and
134 loss on a dated phylogeny of *Drosera*. We tested whether the rates of chromosome evolution
135 differ significantly between *D. subg. Ergaleium* and the other three subgenera, by critically
136 evaluating previously published chromosome counts, verifying voucher specimens to identify
137 possible taxonomic misidentifications, and using BiChrom (binary state linked to chromosome
138 number change) models (Zenil-Ferguson et al., 2017) and Bayes factors to compare models of
139 subgeneric differences in rates of chromosome evolution in a genus-wide phylogenetic context.
140 An ancestral state reconstruction based on the resulting best-fit model was compared with
141 genome size, life history, and centromere type to explore potential factors associated with
142 different chromosome evolution rates between *Drosera* subgenera. Our analyses show highly
143 elevated rates in single chromosome evolution but not polyploidy in *D. subg. Ergaleium*
144 compared to the rest of the genus. Contrary to previous proposals, we found no evidence that
145 such rate shift was due to diploidization after polyploidy or to holocentromeres, pointing to the
146 complexity of factors contributing to rates of single chromosome evolution.
147

148 METHODS

149 **Literature review and evaluation of chromosome counts**

150 Lists of original references for *Drosera* chromosome counts were obtained from the
151 Chromosome Counts Database (Rice et al., 2015), Index of Plant Chromosome Numbers
152 (Goldblatt and Johnson, 1979–), citations referenced by additional publications on karyotypes in
153 *Drosera* (Kondo, 1969; Dawson, 2000; Rivadavia et al., 2003; Veleba et al., 2017), and searches
154 on Google Scholar and the library databases of the University of Minnesota, Curtin University,
155 and University of Western Australia. Voucher specimen information, chromosome count
156 methodology, and provenance data were recorded for every chromosome count identified either
157 from the original publication or from subsequent literature in the case of 14 counts (six
158 publications) where the original data could not be obtained.

159

160 Chromosome counts were excluded from analyses where the chromosome count methodology
161 was flawed or original publication expressed uncertainty about the exact chromosome count (10
162 counts), where counts were made from primary hybrids (25 counts), or if there was taxonomic
163 uncertainty about the material examined (73 counts). Taxonomic uncertainty was characterized
164 by 1) counts that lack both species identification and voucher specimen; 2) species with
165 taxonomy updates after the karyotype publication (especially in the case of species complexes),
166 that lack sufficient provenance or character description and any voucher specimen with which to
167 assign the taxon to the updated species name; 3) counts made from cultivated material of a
168 species often misidentified in cultivation; or 4) a mismatch between the voucher specimen and
169 the name associated with the count. See Supplemental Information S1 for details on evaluating
170 published chromosome count data.

171

172 For species with two or more chromosome numbers after filtering, the number with the most
173 counts was used for subsequent modeling analyses. For 11 species where multiple chromosome
174 numbers had an equal number of counts, one value was selected at random.

175

176 **Phylogenetic reconstruction for comparative analyses**

177 In order to estimate a chronogram for modeling chromosome number evolution, *rbcL* sequences
178 for *Drosera* species and outgroup taxa for non-core Caryophyllales were retrieved from the
179 GenBank (Table S2). Five sequences were removed due to ambiguous nucleotide sites. The
180 taxonomy for *rbcL* sequences with herbarium vouchers at M and SPF (herbarium acronyms
181 following Index Herbariorum) were updated as noted in Table S2. For species with multiple
182 *rbcL* sequences, the longest sequence was kept.

183

184 Sequences were aligned with default settings using the MAFFT (Katoh and Standley, 2013)
185 plug-in for Geneious version 11.1.5 (Kearse et al., 2012). The ends of sequences that were only
186 present in two outgroup species were trimmed. Priors for molecular dating in BEAST version
187 2.6.4 (Bouckaert et al., 2014) followed previous molecular dating analysis across the
188 Caryophyllales (Yao et al., 2019) using a lognormal relaxed molecular clock and the birth-death
189 model of speciation. For each fossil, the prior node was constrained to a lognormal distribution
190 with a mean of 1.0, a standard deviation of 0.5, and an offset based on the age of the fossil. As in
191 Yao et al. (2019), fossil *Aldrovanda intermedia* and *A. ovata* was used to set the prior for the
192 most recent common ancestor (MRCA) of *Dionaea* and *Aldrovanda* with an offset of 41.2 Ma,
193 and *Polygonocarpum johnsonii* was used to constrain the MRCA of the Polygonoideae (in
194 Polygonaceae) included with an offset of 66.0 Ma. The MRCA of non-core Caryophyllales was

195 constrained to 115 Ma with a normal distribution and a standard deviation of 4.0 Ma representing
196 the 95% confidence interval in the posterior distribution of the dating analysis of Yao et al.
197 (2019). The Markov-Chain Monte Carlo (MCMC) was run for 100,000,000 generations,
198 sampling every 1000 generations. The BEAST input file and data are available at
199 10.5281/zenodo.6081366. The resulting summary statistics were visualized in Tracer version
200 1.7.1 (Rambaut et al., 2018). The obtained phylogenetic trees were further reduced to 1 in 10 and
201 summarized in TreeAnnotator version 2.6.2 (Drummond and Rambaut, 2007) with a 10% burn-
202 in, and the maximum clade credibility tree was visualized in FigTree version 1.4.4 (Rambaut,
203 2018). The chronogram (using the ape R package; Paradis and Schliep, 2019) and chromosome
204 count matrices were trimmed to species shared by both datasets for subsequent analyses.
205

206 ***Modeling chromosome number evolution***

207 We used the binary trait linked to chromosome number change model (BiChrom; Zenil-Ferguson
208 et al. 2017) and implemented it in RevBayes software version 1.1.0 (Höhna et al., 2016) to
209 estimate the differences in three rates of chromosome number evolution for each binary state
210 (Fig. 1): γ (a single chromosome gain, by duplication or fission), δ (a single chromosome loss, by
211 rearrangement, fusion, or loss), and ρ (a polyploidy event). The binary state is defined as whether
212 a taxon belongs to *D. subg. Ergaleium* (state E) or not, in which case it belongs to *D. subg.*
213 *Drosera*, *Arcturia*, or *Regiae* (state D). By defining our binary state in this fashion, we estimate a
214 transition rate q , which is a nuisance parameter but allows us to correctly compare rates of
215 chromosome change between the two groups. Species were assigned as state E or state D sensu
216 Fleischmann et al. (2018).
217

218 Our macroevolutionary modeling framework involved simultaneously estimating the rate of
219 evolution of chromosome number and a binary state along a phylogeny. We first defined a
220 matrix describing the instantaneous rate of chromosome number change between two
221 chromosome numbers and between the two states at the same chromosome number (Fig. S1;
222 Mayrose et al., 2010; Zenil-Ferguson et al., 2017). Commonly known as the Q-matrix for
223 continuous time Markov chains, this matrix can be numerically difficult to use because
224 chromosome transition matrices are large and contain many zeros since transitions reflect only
225 single chromosome number changes or doubling (Mayrose et al., 2010; Zenil-Ferguson et al.,
226 2017). These types of matrices are numerically unstable when exponentiated, so limiting the
227 maximum number of chromosomes and rates included is key for estimation (Zenil-Ferguson et
228 al., 2018). Therefore, in our dataset with chromosome number ($2n$) ranging from 8 to 60, we first
229 calculated haploid chromosomes ($1n$) and set the chromosome states for the Q-matrix ranging
230 from 1 to 35 and a bin for 35+ haploid chromosomes to make the matrix more computationally
231 stable (Fig. S1; Zenil-Ferguson et al., 2017, Zenil-Ferguson et al., 2018). We removed *Drosera*
232 *lanata* ($2n = 19$), to avoid non-integer haploid chromosome numbers, and records of B-
233 chromosomes, as these small satellite chromosomes do not segregate normally during cell
234 division. The resulting matrix had 72 rows and 72 columns reflecting 1 to 35 and 35+
235 chromosome numbers for both states E and D (Fig. S1). Since we expect the chromosome
236 evolution rate in *Drosera* outside of *D. subg. Ergaleium* to be more similar to the rate in most
237 angiosperms, we considered state D the ancestral state and E the derived state and only allowed
238 transitions from state D to state E. The probabilities of the root being 1 to 35+ chromosomes in
239 either state were set equal.
240

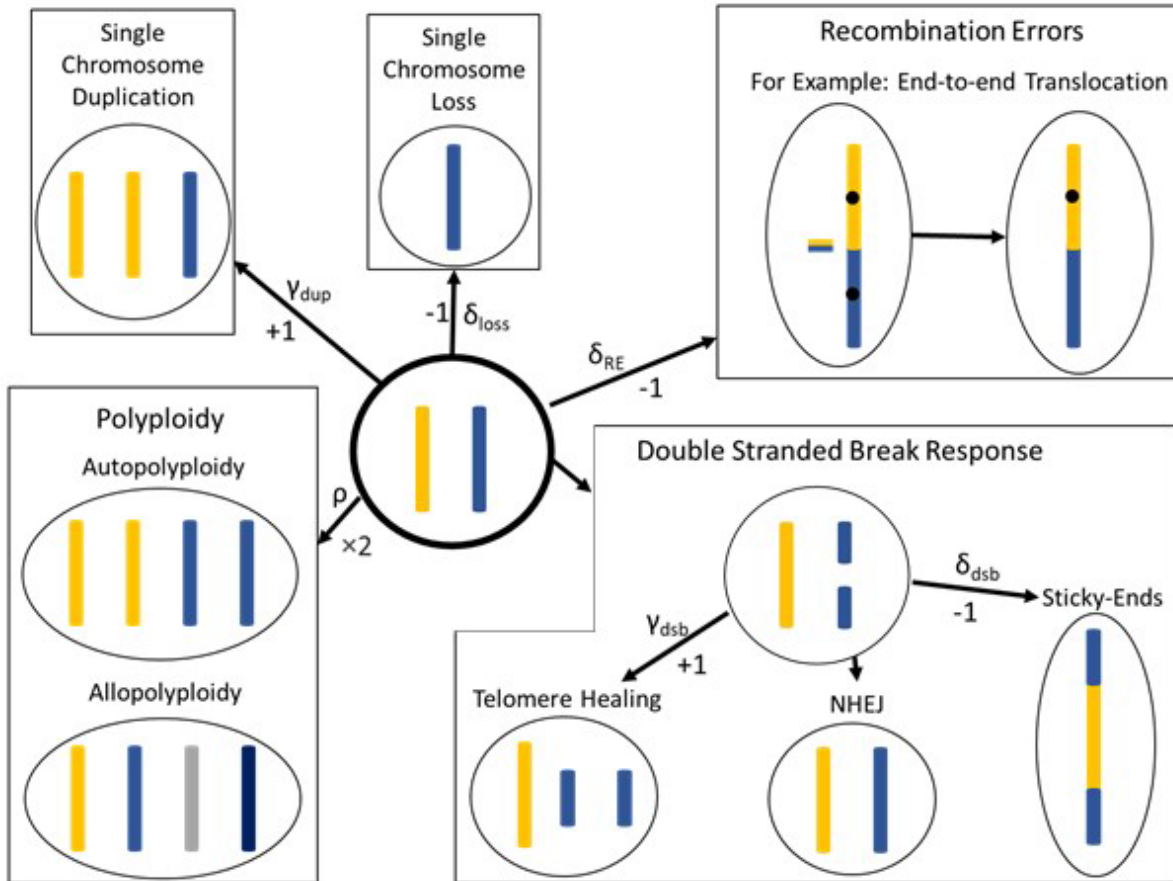


Fig. 1: A summary of the processes that can give rise to changes in chromosome number. Each cell is depicted in haploid form. The original cell (center) starts with two haploid chromosomes. Arrows indicate changes in chromosomes and, where possible, are labelled with the type of change (+1, -1, $\times 2$) and the symbol used in BiChrom models (γ , δ , and ρ respectively; Mayrose & Lysak, 2020). The centromere is shown as a black spot in the recombination error to emphasize the steps required to handle an additional centromere. Since +1 and -1 can occur via multiple mechanisms with different impacts on gene copy number, for example, a subscript is used to distinguish the cause of change. An increase in one chromosome can be due to telomere healing after a chromosome break or a single chromosome duplication; a single chromosome decrease can be due to a recombination error (Nested insertion, end-to-end translocation, or Robertsonian Translocation; Mayrose & Lysak, 2020), two chromosomes fusing after a breakage, or the loss of a single chromosome. Single chromosome loss is unlikely except after polyplody (Luceno & Guerrra, 1996). A doubling of all chromosomes can be due to an auto- or allo-polyplody. Holocentromeres are expected to alleviate issues caused by acentric fragments after double stranded breaks and tangling of bicentric chromosomes after fusion (Cuacos et al., 2015).

241 Three nested models were used for comparison, each with a subset of the rates being constrained
 242 as equal across the two states. The full model (H2) allowed rates (ρ = chromosome doubling, δ =
 243 chromosome loss, γ = chromosome gain) to vary as a function of each of the states D or E. The
 244 fixed-polyplloid model (H1; $\rho_D = \rho_E$) constrained the rate of chromosome doubling to be the same
 245 in D and E. The null model (H0) constrained all rates to be equal for the two states ($\rho_D = \rho_E$, $\gamma_D =$
 246 γ_E , $\delta_D = \delta_E$). Rate priors for all chromosome transitions in both states were set to an exponential
 247 distribution with a mean of 1/3 probability of change per million years (Myr).
 248

249 We ran our custom MCMC scripts in RevBayes (Höhna et al., 2016) for more than 200,000
250 generations until convergence was reached and checked using Tracer (Rambaut et al., 2018). We
251 also verified that effective sample sizes for all the parameters were above 200. Concurrently, we
252 reconstructed ancestral states using marginal posterior probabilities for each of the internal nodes
253 as part of the inference following Freyman and Höhna (2018) and Zenil-Ferguson et al. (2019).
254 The RevBayes input data and scripts are at 10.5281/zenodo.6081366.
255

256 The three models were compared using Bayes factors in RevBayes (Höhna et al., 2016) by
257 calculating power posterior distributions with twenty stepping-stones (Xie et al., 2011). The
258 stepping-stone algorithm was used to calculate the marginal likelihood of each model by
259 estimating the probability of the data between the prior and the posterior. This is done by raising
260 the posterior distribution of the MCMC to a power ranging from 0 to 1, thus providing a discrete
261 approximation between the prior and posterior probabilities. The marginal log likelihoods were
262 calculated from these stepping-stones and were then subtracted to calculate the Bayes factors κ
263 statistic. $\kappa > 6$ is strong evidence in favor of the model input first in the calculation of κ is
264 assumed. If $\kappa > 1$, there is moderate support, and no evidence in favor of either model if κ is
265 between -1 and 1 as described in Kass and Raftery (1995). If κ results in large negative values,
266 the evidence goes in favor of the model whose marginal log-likelihood is subtracting in the
267 calculation of κ .
268

269 All the MCMC outputs were analyzed using Tracer with a burn-in of 10% discarded. The
270 resulting ancestral state reconstruction for the best supported model was visualized with
271 RevGadgets R package (Tribble et al., 2021).
272

273 ***Genome size and mating system***

274 Self-compatibility data for 98 species of *Drosera* were obtained from publications (Table S3).
275 Recent studies (Fleischmann, in press) suggest all *D. auriculata* are self-compatible contrary to a
276 (doubtful) previously-published report by Chen et al. (1997). *Drosera* genome sizes were
277 obtained from Veleba et al. (2017), or newly generated in this study for 17 species at the Flow
278 Cytometry Core Lab at the Benaroya Research Institute (Seattle, WA, U.S.A.). Source, voucher,
279 and size standards used for generating new flow cytometry data are listed in Table S3.
280

281 **RESULTS**

282 ***Chromosome Counts for 127 Drosera species show distinctive patterns of variation between D.*** 283 ***subgenus Ergaleium and other subgenera***

284 An initial dataset of 676 chromosome counts in *Drosera* from 150 species or hybrids were
285 compiled (Table S1). After removing hybrids and low-quality counts, 510 counts from 127
286 species were used for downstream analyses (ca. 48% of all species). These counts included 32%
287 of named species from Africa, 45% from South America, 51% from Australia, 60% from Asia,
288 and all species from North America and Europe. *Drosera* subg. *Arcturia*, *Drosera*, *Ergaleium*,
289 and *Regiae* had respectively 50%, 43%, 51%, and 100% of species with counts.
290

291 Almost every even chromosome number from $2n = 6$ to 46 was reported from *D.* subg.
292 *Ergaleium*, including within-species variation. In contrast, *D.* subg. *Drosera* has chromosome
293 numbers from $2n = 16$ to 80 with variation primarily in polyploid series ($2n = 20, 40, 60, 80$; Fig.

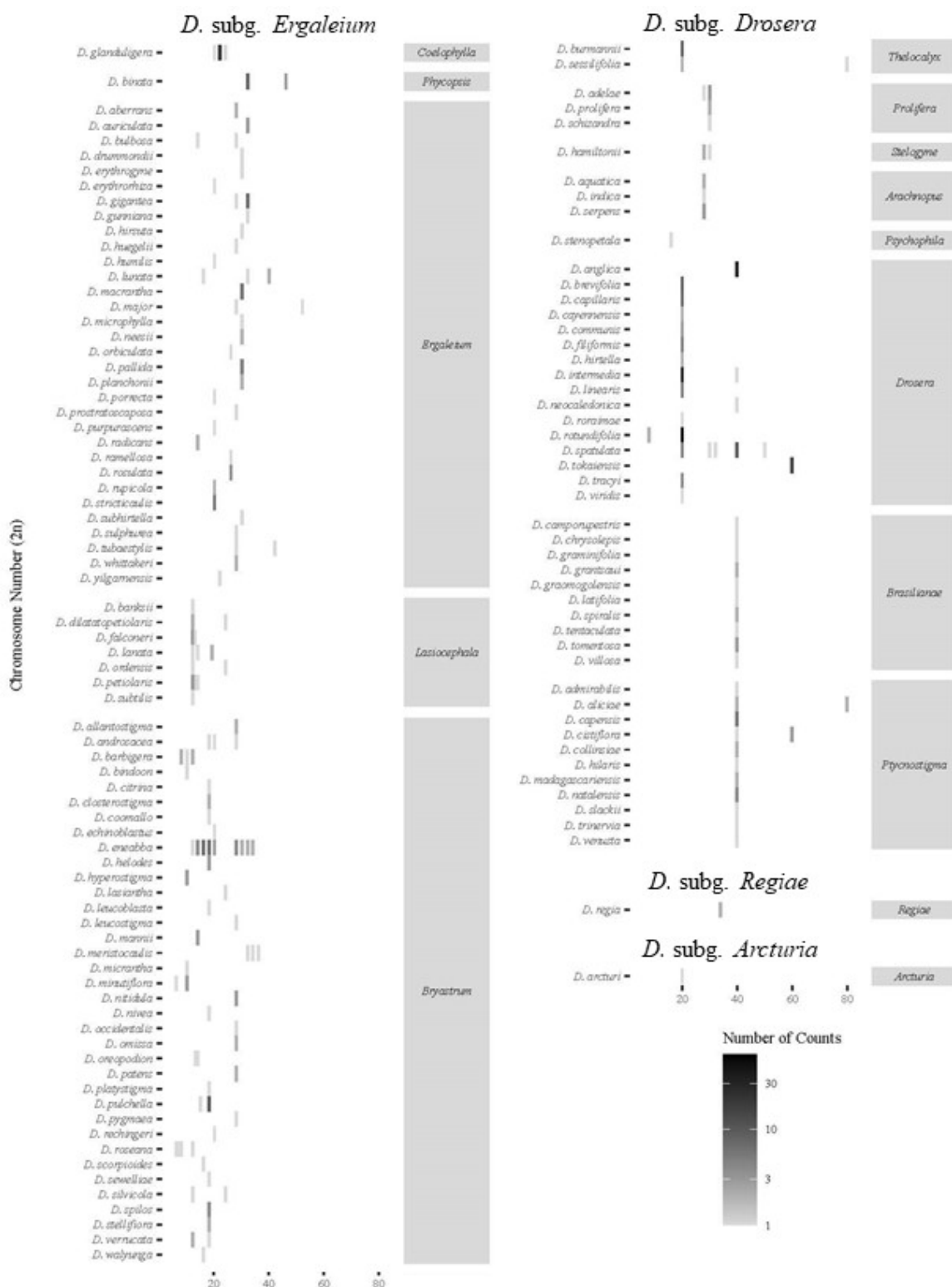


Fig. 2: *Drosera* subg. *Ergaleium* (left) exhibits marked chromosome variation within sections, and even within species. Little within species or within section variation was observed for *D. subg. Drosera* (right), and where variation was observed it fell primarily into polyploidy series. The shade of the square indicates the number of samples for each species, emphasizing that the lack of variation within *D. subg. Drosera* is not due to a lack of samples.

295 2). Chromosome number for *D. arcturi* (*D. subg. Arcturia*) was $2n = 20$ and for *D. regia* (*D.*
296 *subg. Regiae*) was $2n = 34$ (Fig. 2; Table S1).

297

298 **Chronogram Reconstruction**

299 The trimmed *rbcL* matrix included 1,440 bases with 478 variable sites across the 17 outgroup
300 and 79 ingroup taxa. After burn-in, the ESS in BEAST was greater than 200 for all continuous
301 statistics. The *rbcL* tree placed *D. regia* and *D. arcturi* in a clade with *Aldrovanda* and *Dionaea*
302 that was sister to the rest of *Drosera* with strong to moderate support, likely due to long-branch
303 attraction. BEAST analysis estimated the crown age of *D. subg. Ergaleium* at 52.0 Mya and *D.*
304 *subg. Drosera* at 49.6 Mya (Fig. S2).

305

306 ***Drosera* subgenus Ergaleium differs from other subgenera in chromosome evolution rate**

307 We had available chromosome counts and phylogenetic *rbcL* data for 59 species: 25 species
308 from *D. subg. Ergaleium*, 32 species from *D. subg. Drosera*, and one species each from *D. subg.*
309 *Arcturia* and *D. subg. Regiae*. The BiChrom analysis for the full model with all rates estimated
310 separately between *D. subg. Ergaleium* and the other subgenera (H2) took over 200,000
311 generations to converge as the posterior distribution was bimodal.

312

313 In the full model (H2), the mean of the posterior probabilities of gaining ($\gamma_E = 0.23$) or losing (δ_E
314 = 0.25) one chromosome in *D. subg. Ergaleium* was 8.8-fold and 40.3-fold higher than other
315 subgenera ($\gamma_D = 0.026$; $\delta_D = 0.0062$; Table S4; Fig. 3). These rates are interpreted as the amount
316 of single chromosome change per million years. However, the rate of chromosome gain for *D.*
317 *subg. Drosera*, *Arcturia*, and *Regiae* falls within the first quartile of the rate of chromosome gain
318 for *D. subg. Ergaleium* and only the 95% credible interval for the rates of single chromosome
319 loss was distinct (95% HPD $\delta_E = 0.063$ to 0.52; 95% HPD $\delta_D = 6.2 \times 10^{-6}$ to 4.4×10^{-2} ; Table S4;
320 Fig. 3). The rates of polyploidy largely overlapped (Fig. 3).

321

322 Compared to rates estimated in the full model, the null model (H0) estimated an intermediate rate
323 for losing one chromosome, while the estimated rate of polyploidy doubled and the rate for
324 gaining a chromosome decreased (Fig. 3). Comparing Bayes factors for the full model and null
325 model found that the full model had strong support ($BF = 13.5$), showing supporting evidence
326 that there are differences between *D. subg. Ergaleium* and the other subgenera.

327

328 **Rate of polyploidy does not differ among *Drosera* subgenera**

329 Given the very similar inferred chromosome doubling rates for all the subgenera and the
330 genomic instability and potential chromosome loss post a polyploidy event, we tested an
331 additional model estimating chromosome loss and gain for the two groups separately but
332 polyploidy together (H1). The MCMC run for H1 had an effective sampling size above 200 for
333 all statistics and solved issues with the bimodality found in model H2. We found a moderate
334 preference for H1 over the full model (H2; $BF = 5.1$; Table S4; Fig. 3).

335

336 The best fit model (H1) with both chromosome loss (δ) and gain (γ) as functions of each of the
337 subgenera showed higher chromosome loss and chromosome gain rates in *D. subg. Ergaleium*
338 and 95% credible intervals similar to the full model (Table S4; Fig. 3). The mean δ_E was 389.8-

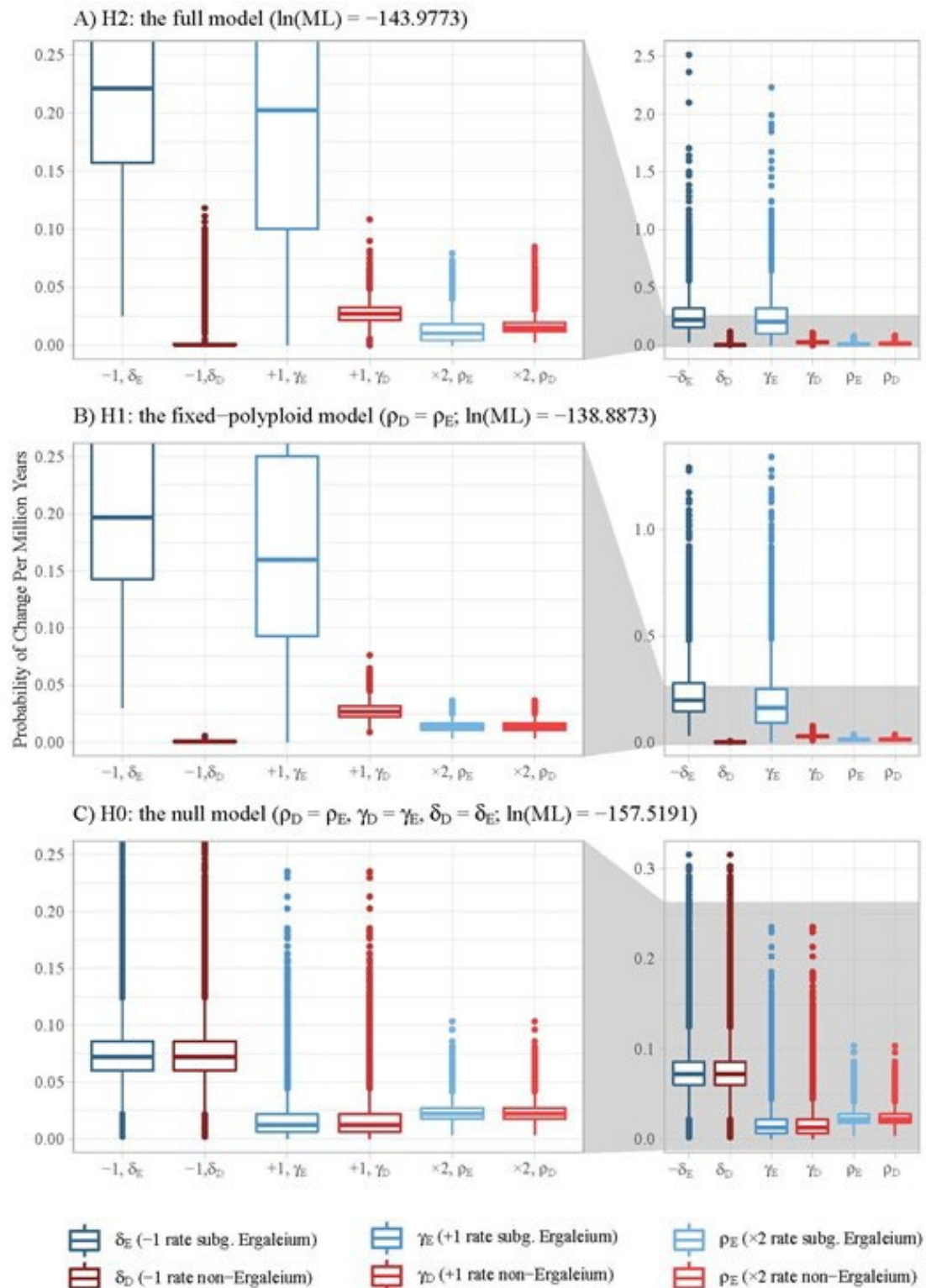


Fig. 3: The posterior sampling distribution from the MCMC after burn-in for (A) H2 where all rates were estimated independently for *Drosera* subg. *Ergaleium* (state E) from the other three *Drosera* subgenera (state D), (B) H1 where all rates were independent except ρ (polypidity) which equal across *Drosera* and (C) H0 where all rates were equal across *Drosera*. δ_D and δ_E are significantly distinct in H2 and H1. All remaining rates were not significantly different between state E and D.

340 fold higher than δ_D and the 95% HPD did not overlap (Table S4; Fig. 3). With overlapping 95%
341 HPDs, the mean γ_E was over 6-fold different than γ_D (Table S4; Fig. 3).

342
343 Under the H1 model, the ancestral state reconstruction estimated the MRCA of *Drosera* to have
344 a haploid chromosome number of eight and state D. The base of *D. subg. Ergaleium* also had a
345 haploid chromosome number of eight but with state E. The difference in single chromosome
346 change between subgenera is supported across the reconstruction by the stability of chromosome
347 number in *D. subg. Drosera* and repeated changes in *D. subg. Ergaleium*. Based on the
348 reconstruction, polyploidization events occurred five times in *D. subg. Ergaleium*, three times in
349 *D. subg. Drosera*, and once in *D. subg. Regiae* (Fig. 4).

350

351 ***Self-compatibility differs between Drosera subgenera***

352 In *D. subg. Ergaleium*, 48 of the 60 (80%) species with known mating systems are self-
353 incompatible in at least some populations (Fig. 4; Table S3.2). In contrast, only three of the 38
354 species (8%) in the remaining three subgenera are self-incompatible, both of them are in *D. subg.*
355 *Drosera* but not closely related (Fig. 4; Table S3.2).

356

357 **DISCUSSION**

358 ***Rates of single chromosome number change significantly differ among Drosera subgenera***

359 After correcting for counting and taxonomic errors and using a model that considers time, the
360 rate of polyploidy in *Drosera* (0.014 per Myr) did not differ between subgenera and was very
361 similar to the polyploidy rate previously reported for perennial angiosperms (0.015 per Myr; Van
362 Drunen and Husband, 2019) and median rate across angiosperm families (0.025 per Myr; Zhan et
363 al., 2021). Similarly, the single chromosome gain (0.027) and loss rate (0.00059) for *Drosera*
364 lineages except *D. subg. Ergaleium* fell higher and lower, respectively, than the average rate
365 (0.0061 and 0.016 respectively) across angiosperm families (Zhan et al., 2021). In contrast, the
366 rate of single chromosome shifts in *D. subg. Ergaleium* was 6-fold (chromosome gain) and 350-
367 fold (chromosome loss) higher than in the remainder of the genus, and the rates of *D. subg.*
368 *Ergaleium* are likely even higher with increased species sampling. Orders of magnitude
369 differences in chromosome loss and gain rates have also been documented between herbaceous
370 versus woody plants, among some *Carex* lineages and among some insect lineages (Escudero et
371 al., 2014; Zenil-Ferguson et al., 2017; Ruckman et al., 2020; Sylvester et al., 2020).

372

373 Elevated rates of single chromosome evolution can be due to increased rates of polyploidy and
374 subsequent rediploidization (Mandáková and Lysák, 2018). However, we found no difference in
375 rates of polyploidy among subgenera in *Drosera*. Although polyploid species in *D. subg.*
376 *Drosera* were considered stable polyploids as their chromosome numbers follow polyploid series
377 (Hoshi and Kondo, 1998; Shirakawa, Hoshi, et al., 2011), we found evidence for genome
378 downsizing after polyploidy across *Drosera*. Of the nine polyploidy events inferred, the most
379 recent (ca. 3.3 Mya) has a genome size close to double that of the sister lineage, while the
380 remaining eight more ancient polyploid lineages have similar or, in seven cases, smaller genome
381 sizes than their diploid sister lineages (Fig. 4; Table S3.1; Veleba et al., 2017). Therefore, both
382 the rate of polyploidy and the post-polyploidy diploidization show similar patterns across
383 *Drosera* and no evidence supports either being the major cause in single chromosome number
384 shifts in *Drosera*.

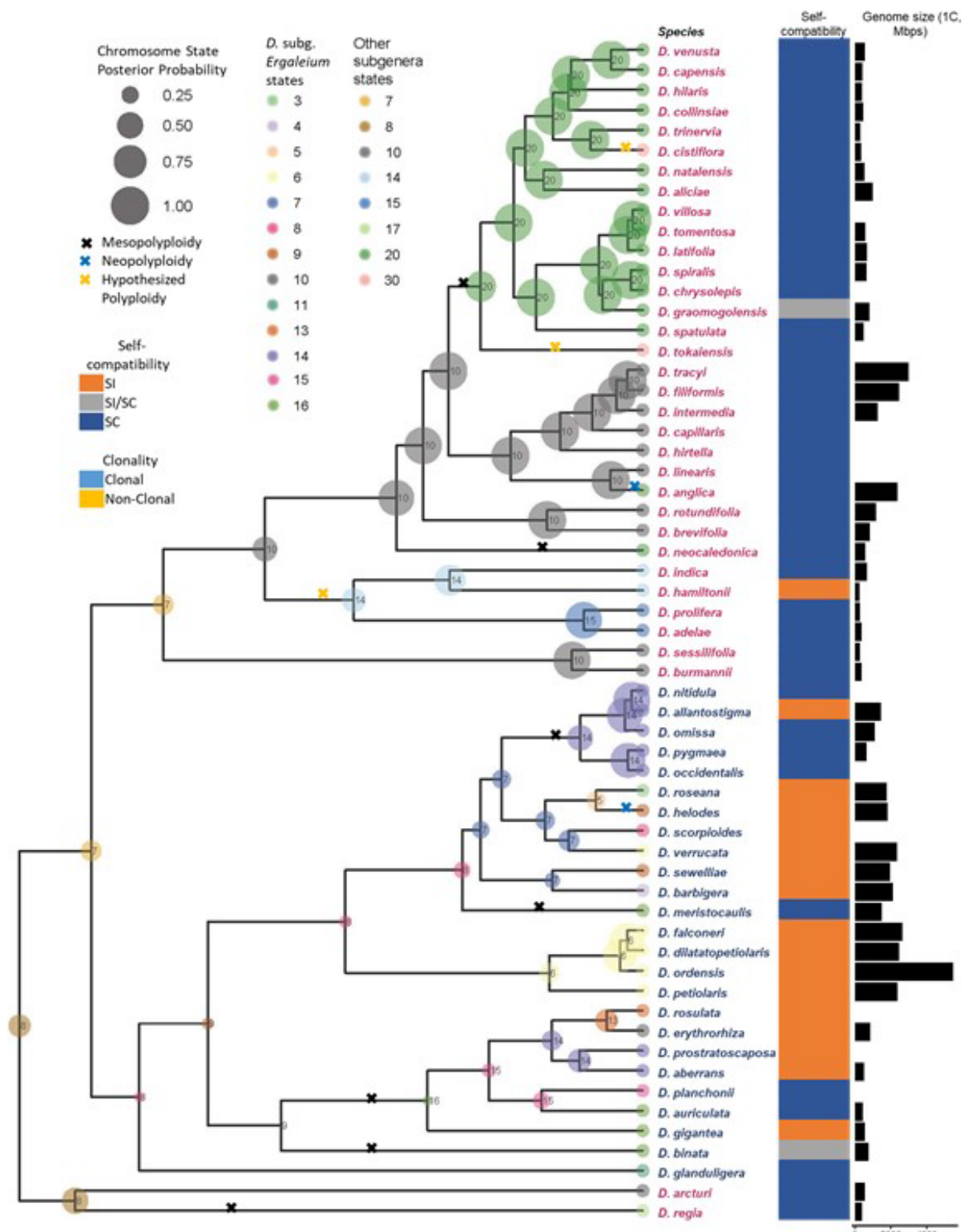


Fig. 4: In addition to having higher rates of single chromosome change, *Drosera* subg. *Ergaleium* (species name in blue) have more species that reproduce clonally and are self-incompatible than the other three subgenera (species name in red). Most polyploid lineages have smaller genome sizes than their diploid sister lineages (marked with a black \times on tree). Numbers and colored bubbles on nodes and tips were ancestral state reconstruction of the chromosome numbers and binary state. Size of bubbles indicate the posterior probability of number. Clonality (occurring in a section with a structure for reproducing genetically identical individuals), self-incompatibility (the ability or inability to produce viable offspring when crossed with itself), and diploid genome size were presented to the right of the species names. Polyploidy as seen by chromosome complete doubling (older and smaller genomes than sister lineages: black \times ; recent and equal too or bigger than sister lineages: blue \times) and 1.5 duplication (yellow \times) were marked on branches.

386

387 While the chromosome loss rates were clearly distinct between *D. subg. Ergaleium* and the other
388 subgenera, the credible intervals for chromosome gain rates overlapped. Our analysis included
389 23% of the named species. To narrow the credible intervals, it is critical for future molecular and
390 cytological work to include proper vouchers, locality information, the number of cells, and
391 individuals counted.

392

393 ***Towards drivers of chromosome evolution rate shift***

394 Holocentromeres have been associated with increased chromosome fission producing a higher
395 number of smaller chromosomes (Cuacos et al., 2015; Ruckman et al., 2020) as chromosome
396 fragments with centromeres can pair and segregate properly even in heterozygous individuals
397 (Luceño and Guerra, 1996; Jankowska et al., 2015; Ruckman et al., 2020). So far, no
398 experimental evidence supports *D. subg. Ergaleium* having a distinct centromere type from the
399 rest of the genus. This lack of association between holocentromeres and significant differences in
400 chromosome evolution rates was also documented in insects (Ruckman et al., 2020).

401

402 A newly formed karyotype may be eliminated due to drift or selection against the deleterious
403 nature of heterozygous individuals, especially in monocentric plants (Husband et al., 2013).
404 Species with means of reproductive assurances (clonal propagation, selfing, etc.) may avoid
405 these issues as the proportion of individuals in the population with the new chromosome number
406 can increase without producing heterozygous individuals (Husband et al., 2013; Van Drunen and
407 Husband, 2019; Spoelhof, Keeffe, et al., 2020). While a perennial life history and clonal
408 propagation are common across *Drosera* (Fleischmann et al. 2018), contrary to expectation, a
409 higher percentage of species studied in *D. subg. Ergaleium* are self-incompatible compared to
410 the other subgenera (Fig 4; Table S3). Interestingly, Spoelhof, Keeffe, et al. (2020) proposed that
411 sexual reproduction (especially outcrossing) is important for the long-term maintenance of
412 species diversity after the formation of a new karyotype.

413

414 Moving forward, exploring the factors that are typically considered within a single species, such
415 as population size, spatial distribution, and meiotic drive, would help dissect the mechanisms
416 underlie new karyotype establishment and macroevolutionary diversification in *Drosera* and
417 beyond (Reed et al., 2013; Bureš and Zedek, 2014; Blackmon et al., 2019; Ruckman et al., 2020;
418 Spoelhof, Soltis, et al., 2020; Griswold, 2021).

419

420 **Conclusion**

421 Differences in chromosome number variation between *Drosera* subg. *Ergaleium* and *D. subg.*
422 *Drosera*, *Arcturia*, and *Regiae* result from significant differences in single chromosome
423 evolution rate rather than sampling bias, chromosome counting errors, or clade age. *D. subg.*
424 *Ergaleium* not only exhibits highly accelerated single chromosome evolution but also a higher
425 percentage of self-incompatible species. Future work on both the natural history and molecular
426 fronts are needed to tease apart the mechanisms underlying the highly elevated rate of single
427 chromosome change. More broadly, our findings illustrate that additional factors other than
428 genome downsizing after polyploidy and holocentromeres impact the rate of single chromosome
429 evolution.

430

431 **SUPPLEMENTAL MATERIALS:**

432 Figure S1: The transition matrix. See Fig. 1 for definition of chromosome transition parameters.
433 Q_{10} is the transition state from state 1 to state 0.
434 Figure S2: The dated *rbcL* phylogeny with all taxa included from the BEAST analysis. Bars on
435 nodes represent the 95% HPD intervals for the age of the node.
436 Table S1: The chromosome count data matrix with notes. Table S1.1 is the matrix itself, Table
437 S1.2 contains the headers and information, and Table S1.3 contains the references for all the
438 data.
439 Table S2: Source for *rbcL* sequences (Table S2.1) including the species name used, the GenBank
440 ID, the originally reported species name, and the reason for taxonomic change if applicable. The
441 species authority for each *Drosera* species (Table S2.2)
442 Table S3: The genome size (Table S3.1), self-compatibility (Table S3.2), and reference (Table
443 S3.3). The genome size matrix included species names, locality and voucher information (visit
444 10.5281/zenodo.6081366 for photo vouchers), control, and reference. The self-compatibility data
445 included species, reference, and notes on changes in taxonomy.
446 Table S4: Table S4.1 shows the marginal log likelihood; estimated rate of chromosome loss (δ),
447 gain (γ), and polyploidy (ρ) for both state E (*Drosera* subg. *Ergaleium*) and state D (the other
448 three *Drosera* subgenera); and the transition from state D to state E for three models. In the full
449 model (H2) all the rates are estimated independently. Table S4.2 contains the 95% HPD
450 distributions for the three models.
451 Supplemental Information S1: Methods for the chromosome count scoring and filtering.
452

453 REFERENCES:

454 Baniaga, A. E., H. E. Marx, N. Arrigo, and M. S. Barker. 2019. Polyploid plants have faster rates
455 of multivariate niche differentiation than their diploid relatives. *Ecology Letters* 23: 68–78.
456 Bennett, S. T., and M. Cheek. 1990. The cytology and morphology of *Drosera slackii* and its
457 relatives in South Africa. *Kew Bulletin* 45: 375–381.
458 Blackmon, H., J. Justison, I. Mayrose, and E. E. Goldberg. 2019. Meiotic drive shapes rates of
459 karyotype evolution in mammals. *Evolution* 73: 511–523.
460 Bouckaert, R., J. Heled, D. Kühnert, T. Vaughan, and C.-H. Wu. 2014. BEAST 2: A software
461 platform for Bayesian evolutionary analysis. *PLoS Comput Biol* 10: 1003537.
462 Bureš, P., and F. Zedek. 2014. Holokinetic drive: centromere drive in chromosomes without
463 centromeres. *Evolution* 68: 2412–2420.
464 Chen, L. 1998. Chromosome numbers, breeding systems and genetic diversity in several species
465 of *Drosera* (Droseraceae) from the south-west of Western Australia. unpublished PhD
466 Thesis, The University of Western Australia.
467 Chen, L., S. H. James, and H. M. Stace. 1997. Self-incompatibility, seed abortion and clonality
468 in the breeding systems of several Western Australian *Drosera* species (Droseraceae).
469 *Australian Journal of Botany* 45: 191.
470 Coghlan, A., E. Eichler, S. Oliver, A. Paterson, and L. Stein. 2005. Chromosome evolution in
471 eukaryotes: a multi-kingdom perspective. *Trends in Genetics* 21: 673–682.
472 Coyne, J. A., and H. A. Orr. 2004. *Speciation*. Sinauer Associates, Inc., Sunderland.
473 Cuacos, M., H. Franklin, F. Chris, and S. Heckmann. 2015. Atypical centromeres in plants—
474 what they can tell us. *Frontiers in Plant Science* 6: 913.
475 Dawson, M. I. 2000. Index of chromosome numbers of indigenous New Zealand
476 spermatophytes. *New Zealand Journal of Botany* 38: 47–150.
477 Demidov, D., V. Schubert, K. Kumke, O. Weiss, R. Karimi-Ashtiyani, J. Buttler, S. Heckmann,

478 et al. 2014. Anti-phosphorylated histone H2AThr120: a universal microscopic marker for
479 centromeric chromatin of mono- and holocentric plant species. *Cytogenetic and genome*
480 *research* 143: 150–156.

481 Dong, Q., and F. Han. 2012. Phosphorylation of histone H2A is associated with centromere
482 function and maintenance in meiosis. *The Plant Journal* 71: 800–809.

483 Drummond, A. J., and A. Rambaut. 2007. BEAST: Bayesian evolutionary analysis by sampling
484 trees. *BMC Evolutionary Biology* 7: 1–8.

485 Van Drunen, W. E., and B. C. Husband. 2019. Evolutionary associations between polyploidy,
486 clonal reproduction, and perenniability in the angiosperms. *New Phytologist* 224: 1266–1277.

487 Escudero, M., S. Martín-Bravo, I. Mayrose, M. Fernández-Mazuecos, O. Fiz-Palacios, A. L.
488 Hipp, M. Pimentel, et al. 2014. Karyotypic changes through dysploidy persist longer over
489 evolutionary time than polyploid changes. *PLoS ONE* 9: e85266.

490 Fleischmann, A. (in press). Flower biology of the carnivorous sundews (*Drosera*, Droseraceae).
491 *Frontiers in Plant Science* (in press).

492 Fleischmann, A., A. T. Cross, R. Gibson, P. M. Gonella, and K. W. Dixon. 2018. Systematics
493 and evolution of Droseraceae. In A. Ellison, and L. Adamec [eds.], *Carnivorous Plants:
494 Physiology, Ecology, and Evolution*, 45–57. Oxford University Press, Oxford.

495 Freyman, W. A., and S. Höhna. 2018. Cladogenetic and anagenetic models of chromosome
496 number evolution: A Bayesian model averaging approach. *Systematic Biology* 67: 195–215.

497 Furuta, T., and K. Kondo. 1999. Effects of gamma-rays on diffused-centromeric chromosomes of
498 *Drosera falconerii* [sic] in vitro. *Chromosome Science* 3: 93–100.

499 Goldblatt, P., and D. E. Johnson [eds.]. 1979–. *Index to plant chromosome numbers*. Missouri
500 Botanical Garden, St. Louis.

501 Grant, V. 1981. *Plant Speciation*. Columbia University Press.

502 Griswold, C. K. 2021. The effects of migration load, selfing, inbreeding depression, and the
503 genetics of adaptation on autotetraploid versus diploid establishment in peripheral habitats.
504 *Evolution* 75: 39–55.

505 Höhna, S., M. J. Landis, T. A. Heath, B. Boussau, N. Lartillot, B. R. Moore, J. P. Huelsenbeck,
506 and F. Ronquist. 2016. RevBayes: Bayesian phylogenetic inference using graphical models
507 and an interactive model-specification language. *Systematic Biology* 65: 726–736.

508 Hoshi, Y., and K. Kondo. 1998. Chromosome differentiation in *Drosera*, subgenus *Rorella*,
509 section *Rossolis*. *Cytologia* 63:199-211

510 Huie, L. 1897. Changes in the cell-organs of *Drosera rotundifolia* produced by feeding with egg-
511 albumen. *Quarterly Journal of Microscopical Science* 39: 387–425.

512 Husband, B. C., S. J. Baldwin, and J. Suda. 2013. The incidence of polyploidy in natural plant
513 populations: major patterns and evolutionary processes. In I. J. Leitch, J. Greilhuber, J.
514 Dolezel, and J. F. Wendel [eds.], *Plant Genome Diversity*, 255–276. Springer.

515 Jankowska, M., J. Fuchs, E. Klocke, M. Fojtová, P. Polanská, J. Fajkus, V. Schubert, and A.
516 Houben. 2015. Holokinetic centromeres and efficient telomere healing enable rapid
517 karyotype evolution. *Chromosoma* 124: 519–528.

518 Kass, R. E., and A. E. Raftery. 1995. Bayes factors. *Journal of the American Statistical
519 Association* 90: 773–795.

520 Katoh, K., and D. M. Standley. 2013. MAFFT multiple sequence alignment software version 7:
521 improvements in performance and usability. *Molecular biology and evolution* 30: 772–80.

522 Kearse, M., R. Moir, A. Wilson, S. Stones-Havas, M. Cheung, S. Sturrock, S. Buxton, et al.
523 2012. Geneious basic: An integrated and extendable desktop software platform for the

524 organization and analysis of sequence data. *Bioinformatics* 28: 1647–1649.

525 Kolodin, P., H. Cempírková, P. Bureš, L. Horová, A. Veleba, J. Francová, L. Adamec, and F.

526 Zedek. 2018. Holocentric chromosomes may be an apomorphy of Droseraceae. *Plant*
527 *Systematics and Evolution* 304: 1289–1296.

528 Kondo, K. 1969. Chromosome numbers of carnivorous plants. *Bulletin of the Torrey Botanical*
529 *Club* 96: 322–328.

530 Kondo, K., and S. Nontachaiyapoom. 2008. An evidence on diffused centromeres in *Drosera*
531 chromosomes provided by scanning electron microscopy. *Chromosome Botany* 3: 79–81.

532 Kress, A. 1970. Zytotaxonomische Untersuchungen an einigen Insektenfängern (Droseraceae,
533 Byblidaceae, Cephalotaceae, Roridulaceae, Sarraceniaceae). *Berichte der Deutschen*
534 *Botanischen Gesellschaft* 83: 55–62.

535 Luceño, M., and M. Guerra. 1996. Numerical variations in species exhibiting holocentric
536 chromosomes: a nomenclatural proposal. *Caryologia* 49: 301–309.

537 Mandáková, T., and M. A. Lysak. 2018. Post-polyploid diploidization and diversification
538 through dysploid changes. *Current Opinion in Plant Biology* 42: 55–65.

539 Mayrose, I., M. S. Barker, and S. P. Otto. 2010. Probabilistic models of chromosome number
540 evolution and the inference of polyploidy. *Syst. Biol.* 59: 132–144.

541 Mayrose, I., S. Zhan, C. Rothfels, K. Magnuson-Ford, M. Barker, L. Rieseberg, and S. Otto.
542 2011. Recently formed polyploid plants diversify at lower rates. *Science* 333: 1257.

543 Mayrose, I., and M. A. Lysak. 2020. The evolution of chromosome numbers: mechanistic
544 models and experimental approaches. *Genome Biology and Evolution* 13: evaa220

545 Nakamura, T., and K. Ueda. 1991. Phytogeography of Tokai Hilly Land Element II. Taxonomic
546 study of *Drosera tokaiensis* (Komiy & C. Shibata) T. Nakamura & Ueda (Droseraceae).
547 *Acta phytotaxonomica et geobotanica* 42: 125–137.

548 Nontachaiyapoom, S., S. Inaga, A. Iino, and K. Kondo. 2000. Ultrastructure of chromatin
549 organization in diffused-centromeric chromosomes of *Drosera* as compared to localized-
550 centromeric chromosomes of *Drosophyllum* (Droseraceae) detected by scanning electron
551 microscopy. *Chromosome Science* 4: 75–85.

552 Paradis E. & Schliep K. 2019. ape 5.0: An environment for modern phylogenetics and
553 evolutionary analyses in R. *Bioinformatics* 35: 526–528.

554 Rambaut, A. 2018. FigTree v. 1.4.4. Website <http://tree.bio.ed.ac.uk/software/figtree/> [accessed
555 18 June 2021].

556 Rambaut, A., A. J. Drummond, D. Xie, G. Baele, and M. A. Suchard. 2018. Posterior
557 Summarization in Bayesian phylogenetics using Tracer 1.7. *Systematic Biology* 67: 901–
558 904.

559 Reed, F. A., A. Traulsen, and P. M. Altrock. 2013. Underdominance. *Brenner's Encyclopedia of*
560 *Genetics: Second Edition*: 247–249.

561 Rice, A., L. Glick, S. Abadi, M. Einhorn, N. M. Kopelman, A. Salman-Minkov, J. Mayzel, et al.
562 2015. The Chromosome Counts Database (CCDB) – a community resource of plant
563 chromosome numbers. *New Phytologist* 206: 19–26.

564 Rivadavia, F. 2005. New chromosome numbers for *Drosea* L. (Droseraceae). *Carnivorous Plant*
565 *Newsletter* 34: 85–91.

566 Rivadavia, F., K. Kondo, M. Kato, and M. Hasebe. 2003. Phylogeny of the sundews, *Drosera*
567 (Droseraceae), based on chloroplast *rbcL* and nuclear 18S ribosomal DNA sequences.
568 *American Journal of Botany* 90: 123–130.

569 Rivadavia, F., V. F. O. De Miranda, G. Hoogenstrijd, F. Pinheiro, G. Heubl, and A. Fleischmann.

570 2012. Is *Drosera meristocaulis* a pygmy sundew? Evidence of a long-distance dispersal
571 between Western Australia and northern South America. *Annals of Botany* 110: 11–21.

572 Rivero, R., E. B. Sessa, and R. Zenil-Ferguson. 2019. EyeChrom and CCDBcurator: Visualizing
573 chromosome count data from plants. *Applications in Plant Sciences* 7(1): e1207.

574 Román-Palacios, C., Y. F. Molina-Henao, and M. S. Barker. 2020. Polyploids increase overall
575 diversity despite higher turnover than diploids in the Brassicaceae. *Proceedings of the Royal
576 Society B: Biological Sciences* 287.

577 Rosenberg, O. 1903. Das Verhalten der Chromosomen in einer hybriden Pflanze. *Berichte der
578 Deutschen Botanischen Gesellschaft* 21: 110–119.

579 Rothfels, K., and M. Heimburger. 1968. Chromosome size and DNA values in sundews
580 (Droseraceae). *Chromosoma* 25: 96–103.

581 Ruckman, S. N., M. M. Jonika, C. Casola, and H. Blackmon. 2020. Chromosome number
582 evolves at equal rates in holocentric and monocentric clades. *PLOS Genetics* 16: e1009076.

583 Sheikh, S. A., and K. Kondo. 1995. Differential staining with orcein, giemsa, CMA, and DAPI
584 for comparative chromosome study of 12 species of Australian *Drosera* (Droseraceae).
585 *American Journal of Botany* 82: 1278–1286.

586 Sheikh, S. A., K. Kondo, and Y. Hoshi. 1995. Study on diffused centromeric nature of *Drosera*
587 chromosomes. *Cytologia* 60: 43–47.

588 Shirakawa, J., Y. Hoshi, and K. Kondo. 2011. Chromosome differentiation and genome
589 organization in carnivorous plant family Droseraceae. *Chromosome Botany* 6: 111–119.

590 Shirakawa, J., K. Nagano, and Y. Hoshi. 2011. A chromosome study of two centromere
591 differentiating *Drosera* species, *D. regia* and *D. arcturi*. *Caryologia* 64: 453–463.

592 Spoelhof, J. P., R. Keeffe, and S. F. McDaniel. 2020. Does reproductive assurance explain the
593 incidence of polyploidy in plants and animals? *New Phytologist* 227: 14–21.

594 Spoelhof, J. P., D. E. Soltis, and P. S. Soltis. 2020. Habitat Shape Affects Polyploid
595 Establishment in a Spatial, Stochastic Model. *Frontiers in Plant Science* 0: 1770.

596 Stebbins, G. L. 1971. *Chromosome Evolution in Higher Plants*. Edward Arnold Ltd, London.

597 Sylvester, T., C. E. Hjelmen, S. J. Hanrahan, P. A. Lenhart, J. S. Johnston, and H. Blackmon.
598 2020. Lineage-specific patterns of chromosome evolution are the rule not the exception in
599 Polyneoptera insects. *Proceedings of the Royal Society B* 287: 20201388

600 Tribble, C. M., W. A. Freyman, M. J. Landis, J. Y. Lim, J. Barido-Sottani, B. T. Kopperud, S.
601 Höhna, and M. R. May. 2021. RevGadgets: an R Package for visualizing Bayesian
602 phylogenetic analyses from RevBayes. *bioRxiv*: 2021.05.10.443470.

603 Veleba, A., P. Šmarda, F. Zedek, L. Horová, J. Šmerda, and P. Bureš. 2017. Evolution of
604 genome size and genomic GC content in carnivorous holokinetics (Droseraceae). *Annals of
605 Botany* 119: 409–416.

606 Wanner, G., E. Schroeder-Reiter, W. Ma, A. Houben, and V. Schubert. 2015. The ultrastructure
607 of mono- and holocentric plant centromeres: an immunological investigation by structured
608 illumination microscopy and scanning electron microscopy. *Chromosoma* 124: 503–517.

609 Weiss-Schneeweiss, H., K. Emadzade, T.-S. Jang, and G. M. Schneeweiss. 2013. Evolutionary
610 consequences, constraints and potential of polyploidy in plants. *Cytogenetic and Genome
611 Research* 140: 137–150.

612 Windham, M. D., and G. Yatskievych. 2003. Chromosome studies of cheilanthoid ferns
613 (Pteridaceae: Cheilanthoideae) from the western United States and Mexico. *American
614 Journal of Botany* 90: 1788–1800.

615 Xie, W., P. O. Lewis, Y. Fan, L. Kuo, and M. H. Chen. 2011. Improving marginal likelihood

616 estimation for Bayesian phylogenetic model selection. *Systematic Biology* 60: 150–160.
617 Yao, G., J.-J. J. Jin, H.-T. T. Li, J.-B. B. Yang, V. S. Mandala, M. Croley, R. Mostow, et al.
618 2019. Plastid phylogenomic insights into the evolution of Caryophyllales. *Molecular*
619 *Phylogenetics and Evolution* 134: 74–86.
620 Zedek, F., P. Veselý, L. Horová, and P. Bureš. 2016. Flow cytometry may allow microscope-
621 independent detection of holocentric chromosomes in plants. *Scientific Reports* 6: 27161.
622 Zenil-Ferguson, R., J. M. Ponciano, and J. G. Burleigh. 2017. Testing the association of
623 phenotypes with polyploidy: An example using herbaceous and woody eudicots.
624 *Evolution* 71: 1138–1148.
625 Zenil-Ferguson, R., J.G. Burleigh, and J.M. Ponciano, 2018. chromoploid: An R package for
626 chromosome number evolution across the plant tree of life. *Applications in Plant*
627 *Sciences*, 6: p.e1037.
628 Zenil-Ferguson, R., J. G. Burleigh, W. A. Freyman, B. Igić, I. Mayrose, and E. E. Goldberg.
629 2019. Interaction among ploidy, breeding system and lineage diversification. *New*
630 *Phytologist* 224: 1252–1265.
631 Zhan, S. H., S. P. Otto, and M. S. Barker. 2021. Broad variation in rates of polyploidy and
632 dysploidy across flowering plants is correlated with lineage diversification. *bioRxiv*:
633 2021.03.30.436382.
634